مجلة كلية التربية الاساسية
كلية التربية الاساسية – الجامعة المستنصرية
Journal of the College of Basic Education Vol.31 (NO. 134) 2025, pp. 48-68

Synthesis and Nonlinear Optical Properties of Au and ZnO Nanoparticles and Their Nanocomposites

Nadia Mohammed Jassim [(1)]
College of Science, Diyala University, Diyala 4200, Iraq.
nadiajassim@uodiyala.edu.iq

Hanan Khalid Owda [(2)]
College of Science, Diyala University, Diyala 4200, Iraq.
sciphyms232408@uodiyala.edu.iq

Abstract

This Study elaborates on the synthesis and nonlinear optical characteristics of gold (Au) and zinc oxide (ZnO) nanoparticles and nanocomposites (ZnO-Au NCs), which are prepared by pulsed laser ablation in liquid (PLAL) approach. ZnO is a year-wide bandgap semiconductor with high exciton binding energy (60 meV) that is economical, environmentally friendly, and non-toxic thus it is suitable in optical and electronic devices. Characterizations of the synthesized nanoparticles were done by X-ray diffraction (XRD), energy dispersive X-ray (EDX), ultraviolet-visible (UV-Vis) spectroscopy, Fourier-transform infrared (FTIR) spectroscopy, field emission scanning electron microscopy (FESEM), and transmission electron microscopy (TEM). The results show that, ZnO- Au nanocomposites have better nonlinear optical properties than the original Au and ZnO nanoparticles. The nonlinear refractive index (n_2) of ZnO-Au NCs was determined to be 3.27 x 10^4 cm_2 /GW, which is much higher than that of pure ZnO (3.7 x 10^4 cm^2 /GW). Another technique used in the study to obtain the nonlinear optical parameters was the Z-scan in which, it was found that the inclusion of Au in ZnO increases light absorption by the surface plasmon resonance (SPR) effect. The study exudes the potential of ZnO-Au nanocomposites in the future of the design of advanced nonlinear photonic devices and environmental remediation, which is a clean and efficient way of synthesizing functional nanomaterials.

Keyword: Zinc Oxide NPs, Gold Nanoparticles, Nonlinear Optical Properties, Pulsed Laser Ablation.

1. Introduction

Nonlinear optics (NLO) is a research area that deals with optical effects that occur when materials are exposed to intense incident light and which are not linear to their optical behaviour. A common plasma to use in this field is the nanoparticles made by laser ablation due to the nonlinear optical effects occurring with the use of such light (often called the nonlinear optical effect).

During the past ten years, nonlinear optical properties have been explored by numerous researchers because of its potential in applications to optical signal processing, such as all-optical switches at high speed, optical phase-conjugation, and optical limiting (Ganeev, 2019). These properties also have seen great interest in developing several types of photonic devices including lasers, waveguides, all-optical switches, optical gates, detectors, sensors, spectrometers, microscopes, and data storage devices all of which are advantageous because of nonlinear responses and electronic energy gaps (Gündoğdu et al., 2021).

Despite the existing great number of techniques, the use of Z-scan method is one of the simplest and most efficient laboratory methods used to measure the nonlinear optical response of a material (Jassim, 2024). The Z-scan method has two major configurations. The nonlinear refractive index (n_2) and the sign and magnitude of the real and imaginary part of the Third Order NLO response are measured using the closed-aperture Z-scan. Open-aperture Z-scan on the other hand is applied to measure the nonlinear absorption coefficient comprising of reverse saturable absorption (RSA) and saturable absorption (SA). The mathematical principles underlying this approach include the equations of nonlinear phase shift, the effective sample length (Leff), which bring the experimental data related to extracted optical parameters (Jassim et al., 2024).

The gold nanoparticles (Au NPs) have elicited wide attention due to their anomalous optoelectronic and plasmonic characteristics, which render them extremely pertinent in the nonlinear optics, laser physics, and optoelectronics. They have found uses in optical switching, localization, catalysis, plasmonic waveguides, photovoltaics, drug delivery in medical sciences, spectroscopy, nanotechnology, electrochemical analysis and biochemical analysis. The said properties are allied to surface plasmon resonance (SPR) close to 1/530 nm, where linear and nonlinear optical responses are amplified by collective oscillations of the conduction electrons (Ganeev, 2019; Abdulrahman et al., 2022). Zinc oxide (ZnO) is another significant semiconductor being actively researched because it is inexpensive, has a large bandgap (3.37 eV), high exciton binding energy (~60 meV), and has great potential in luminescence (Multian et al., 2017). The numerous applications of ZnO NPs in photocatalysis, gas sensing, biosensors, and optoelectronics are attributed to the special electronic and electro-optical properties (Mostafa, 2021). Pulsed laser ablation in liquid (PLAL) has become a versatile surfactant-free method of preparing nanostructures through ablation of a solid target in liquid. The properties and morphology of the obtained nanomaterials are dependent on

the parameters of the solvent nature, solid target composition, laser wavelength, pulse duration, energy, and focusing conditions (Yogesh et al., 2021). This method has proved to be efficient to make ZnO NPs in different forms and sizes through ablution of a target of zinc metal in water or other solvents (Yao et al., 2021).

The surface to volume ratio of materials at the nanoscale is also very high hence causing drastic changes in the physical and chemical properties of a material in comparison to bulk materials. As an example, Au NPs suspended in a transparent medium and having a diameter smaller than 100 nm are colored in ruby-red, as opposed to metallic gold, which is the collective oscillation of conduction electrons on the surface of a nanoparticle when incited by incident light known as surface plasmon resonance (SPR) (Zhang et al., 2017.)

The present work focuses on the surfactant-free synthesis of Au NPs, ZnO NPs, and ZnO–Au nanocomposites (NCs) using PLAL and on the systematic investigation of their structural and nonlinear optical properties. The novelty of this study lies in demonstrating how the incorporation of Au into ZnO enhances the nonlinear refractive index (n_2) and nonlinear absorption coefficient (β). These results highlight the significance of ZnO–Au NCs for advanced photonic devices and environmental remediation.

2. Experimental Techniques

2.1 Samples preparation

The synthesis of gold nanoparticles (Au NPs), zinc oxide nanoparticles (ZnO NPs), and (ZnO-Au NCs) was carried out using a modified pulsed laser ablation in liquid (PLAL) procedure . For the preparation of Au NPs, a high-purity gold pellet (99.99%) was placed at the bottom of a glass container containing 10 mL of deionized water (DW). The target was irradiated using a Nd:YAG laser operating at a wavelength of 1064 nm, with a pulse duration of 9 ns and a repetition rate of 1 Hz. The laser energy was set to 500 mJ, and the irradiation was continued for 500 pulses. This ablation process resulted in the formation of a ruby-red colloidal solution, confirming the presence of dispersed Au nanoparticles .For the synthesis of ZnO NPs, the same experimental setup was employed, while adjusting the laser energy to 700 mJ and increasing the number of pulses to 750. A zinc target was immersed in 10 mL of deionized water and irradiated under these conditions. The ablation process produced a whitish colloidal suspension attributed to the formation of ZnO nanoparticles. To prepare ZnO-Au NCs, a zinc pellet (98.5% purity) was immersed in the previously synthesized Au colloid. The suspension was subsequently irradiated with the Nd:YAG laser under identical operating

parameters (λ = 1064 nm, 700 mJ, 500 pulses, 9 ns, 1 Hz) .The ablation of the zinc target in the Au colloid resulted in the formation of a ZnO–Au nanocomposite colloidal solution, as shown in Fig .1.

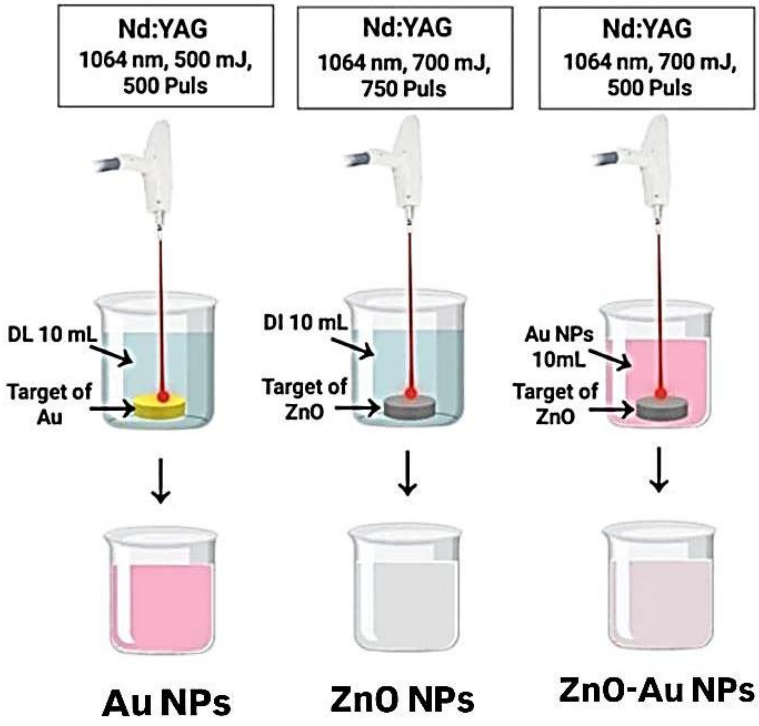

Fig.1 Steps of preparation.

2.2 Z-scan Technique

The Z-scanning technique is divided into two methods: closed-aperture and open-aperture configurations, which are used to calculate nonlinear optical properties such as the nonlinear absorption coefficient (β) and nonlinear refractive index (n_2) of prepared samples. A pulsed Nd:YAG laser with a wavelength of 532 nm was used in this technique. A short-focal-length lens (10 mm) used to focus the light beam, directing the radiation onto the sample along the z-axis, as mentioned in fig.2. The sample was then moved along the z-axis, intersecting with the laser focus positioned at z=0. In the open-aperture configuration, all emitted light was collected by a lens positioned behind the sample, ensuring comprehensive beam capture. A photodetector located after the aperture captured the emitted laser beam. In the closed-aperture mode, a small aperture was placed in front of the detector to measure nonlinear refraction, while in the open-aperture mode, the aperture was removed or opened completely to capture all transmitted light and calculate nonlinear absorption. As the sample was moved along the z-axis, the

transmittance value was measured at each location. The collected data were then processed using standard z-scan methodologies to extract the sample's nonlinear optical properties.

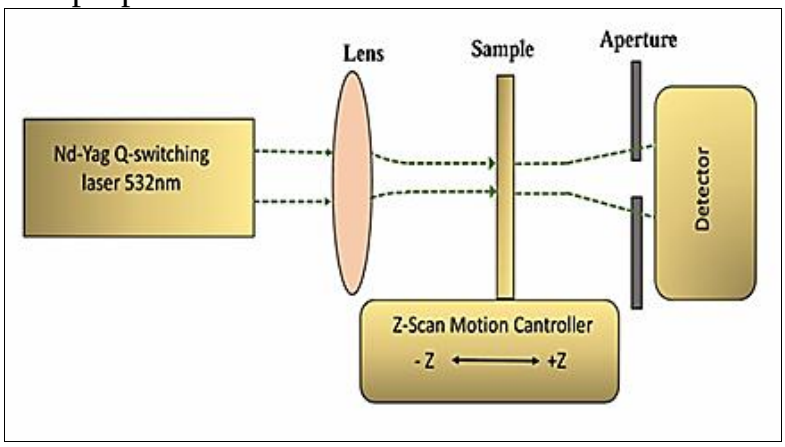

Fig 2. Z-scan experimental setup

2.3 Sample Characterization

Several advanced characterization techniques were used. These tools provided comprehensive insights into the structural, morphological, optical, and elemental properties of the samples. Table 1.1 summarizes the main tools used, along with their objectives and specifications.

Table 1. Details of Measurements devices.

Instrument	Aim
XRD	To study the Structural properties.
Fourier Transform Infrared Spectroscopy (FTIR)	In order to determine the functional groups and bonding.
Field emission scanning electron microscopy (FESEM)	To study the morphology of the surface.
The Transmission electron microscopy(TEM)	To examine the internal structure and particle size.
UV Absorption Spectroscopy	To study the optical properties and bang gap.
Nonlinear optical(Z-Scan)	To investigate the nonlinear optical characteristics of the third order
Energy Dispersive X-ray analysis (EDX)	To determine the elemental composition and confirm the presence of Au, Zn, and O in the nanoparticles.

The nature of the prepared samples, in this study, was determined, by applying various powerful analytical methods, that were accessible in

Baghdad laboratories. The structural aspect was also examined using X-Ray Diffraction (XRD), namely PANalytical X'Pert Pro model that gave it insights into crystallinity and identification of phases of the nanoparticles. Fourier Transform Infrared Spectroscopy (FTIR) was used to analyze the functional groups and chemical bonds by use of Thermo Fisher Scientific Nicolet iS10 model and the results confirmed the interaction between ZnO and Au in the nanocomposites through identification of surface-bound molecules. The samples were also analyzed, with the help of Energy Dispersive X-ray Spectroscopy (EDX), the sample of which was measured with the help of the model Oxford Instruments INCA Energy 350, and it indicated that the samples contained gold, zinc, and oxygen, which proves the purity and proper formation of the nanoparticles. FESEM JEOL JSM-7610F was used to analyze the surface structure and size distribution of the nanoparticles but Transmission Electron Microscopy (TEM) with the model of Hitachi HT7700 was used to provide detailed pictures of the internal structure. All these techniques were used to get detailed information regarding the physical, chemical, and optical characteristics of the nanomaterials.

4. Results And Discussion

The Fig **Fig. (3A**) shows the XRD analysis of (Au NPs) , which reveals the presence of three significant peaks. The diffraction peaks at 2θ = 44.1° relates to (200), 64.5° relates to (220), and 77.6° relates to (311) , denoting the face-centered cubic (FCC) configuration of Au, as per JCPDS card No. 00-004-0784. The clarity, sharpness, and high intensity of the peaks indicate the high crystallinity and good purity of the prepared particles.

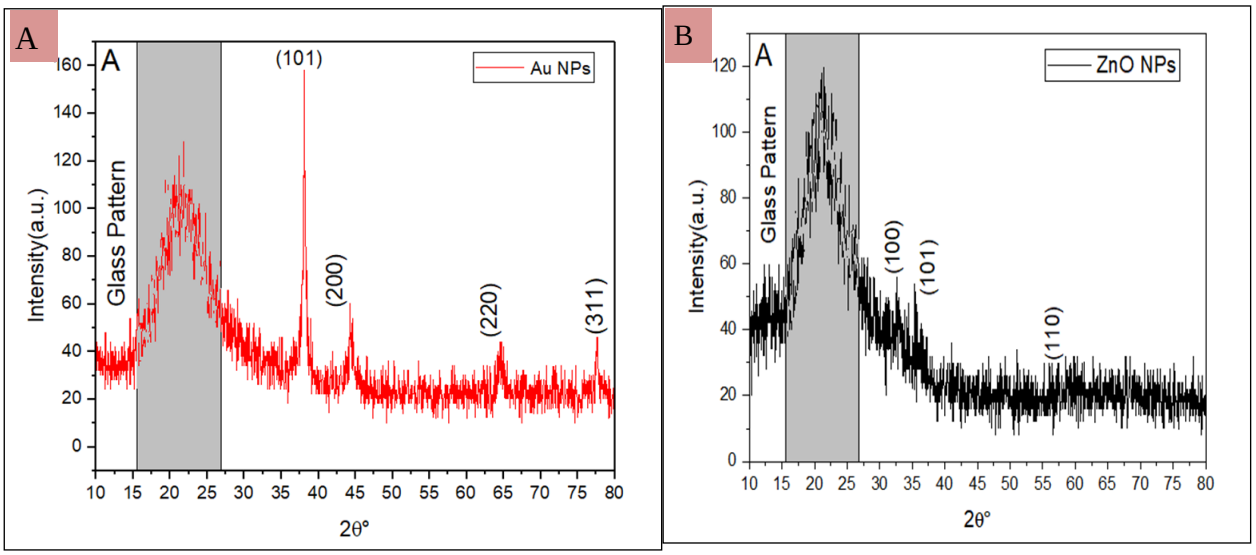

مجلة كلية التربية الاساسية
كلية التربية الاساسية – الجامعة المستنصرية
Journal of the College of Basic Education Vol.31 (NO. 134) 2025, pp. 48-68

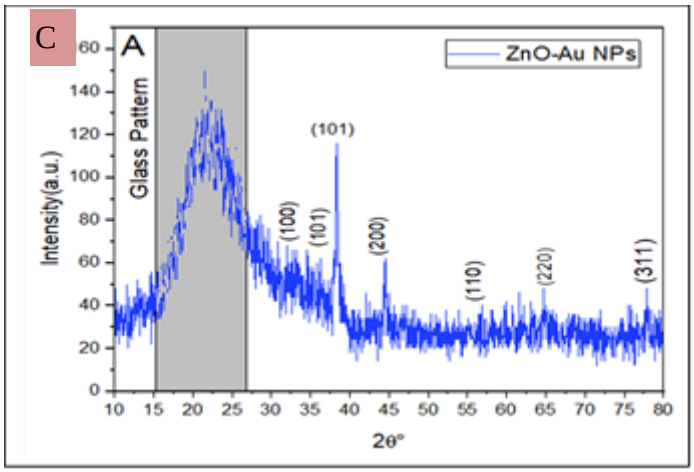

Fig. 3. XRD analysis spectra of (A) Au NPs , (B) ZnO NPs ,(C) ZnO-Au nanocomposites.

For the ZnO nanoparticles in the Fig **Fig. (3B**), peaks appeared at angles 2θ = 31.7°, 36.0°, and 56.2°, which correspond to the (100), (101), and (110) crystal planes, proving that the produced particles had a wurtzite-type hexagonal structure, according to the (JCPDS) standard card No. 01-079-0207. The broadening of the peaks also indicates the small crystal size, which supports the formation of particles on the nanoscale. **Fig. (3C**) illustrates the X-ray diffraction (XRD) pattern of the ZnO-Au nanocomposites sample. The characteristic crystalline peaks appear at locations corresponding to JCPDS cards No. 00-004-0784 for Au and No. 01-079-0207 for ZnO . The peaks observed at about 2θ = 31.7°, 36.0°, and 56.2° correspond to the (100), (101), and (110) crystal planes, respectively, of the hexagonal wurtzite structure of ZnO. Furthermore, additional peaks occur at around 2θ = ~44.1°, 64.5°, and 77.6° which are due to the (200), (220), and (311) structural planes of the FCC (Au) nanostructure. Scherrer's **equation (1)** was used to further compute the Au NPs, ZnO NPs crystallite size D(Ali, et al, 2022),as shown in Table (2) :

$$D = K\lambda / \beta \cos\theta \quad (1)$$

where D indicates the size of the particle, K is Scherrer's constant = 0.9, β denotes full width over half maximum (FWHM) expressed in radians.

Table 2. The Z-scan of closed aperture and change in transmittance.

Samples	Particle Size	Tmax	Tmin	ΔTpv	n2 cm²/GW
Au	30.727	0.74	0.33	0.41	55200
ZnO	27.289	0.61	0.22	0.39	37000
ZnO-Au	27.289	0.40	0.10	0.30	32700

Fig. (4A) shows the EDX spectrum of a sample of Au NPs, in which clear peaks corresponding to pure Au are observed, with no detectable impurities. The results showed weight and atomic ratios of 100%, confirming the purity of the sample and the successful preparation without impurities. **Fig. (4B)** shows the EDX spectrum of the ZnO nanoparticle sample, showing that the sample had clear peaks for zinc and oxygen only, with no impurities. The weight percentage of oxygen was 95.34% compared to 4.66% for zinc, indicating a predominance of oxygen at the surface, which is consistent with the properties of nanoparticles prepared in aqueous medium.

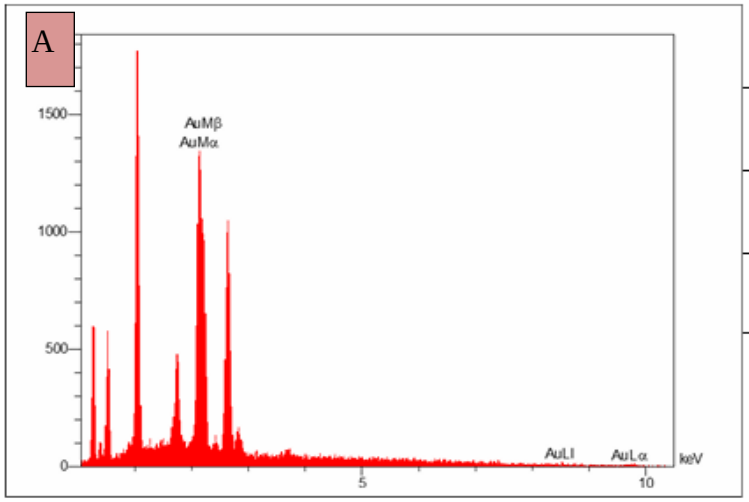

Element	W%	A%
Au	100.00	100.00
Total	100.00	100.00

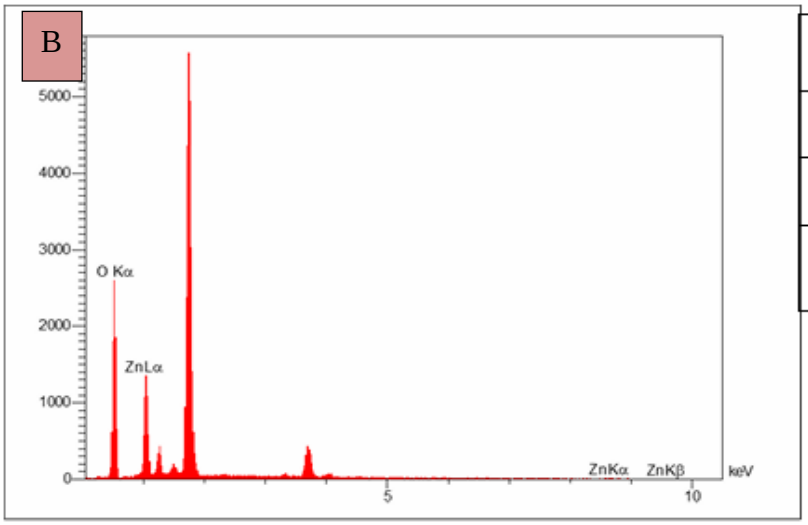

Element	W%	A%
O	95.34	98.82
Zn	4.66	1.18
Total	100.00	100.00

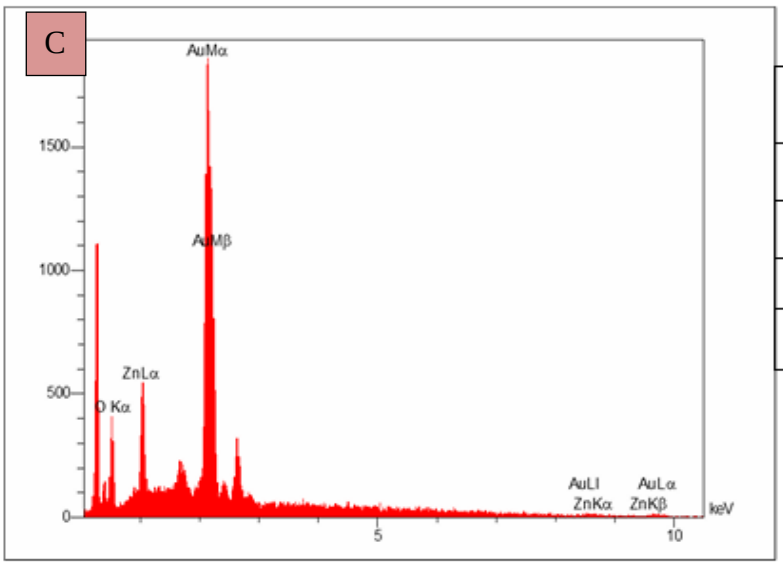

Element	W%	A%
O	43.05	89.54
Zn	2.44	1.18
Au	54.51	9.21
Total	100.00	100.00

Fig. 4. EDX spectrum of A) Au NPs, B) ZnO NPs, C) ZnO-Au nanocomposites.

Fig. (4C) shows the EDX spectrum of the ZnO/Au nanocomposites, which consists of three main elements: oxygen, zinc, and Au. The weight percentage of Au was 54.51%, indicating a high-density deposition of Au particles on the ZnO surface, while the weight percentages of zinc and oxygen were lower. The results suggest significant surface coverage by Au, which may obscure the Zn and O signals.

Fig. (5A) shows a sharp absorption peak at 525 nm, which is a distinctive feature of Au NPs. This peak originates from the surface plasmon resonance (SPR), where the free electrons on the surface of Au NPs oscillate collectively when exposed to light. In addition, another absorption band is observed at around 254 nm, which is attributed to the interband electronic transitions of Au.

Fig. (5B) The peak at wavelength 342 nm for zinc nanoparticles due to electronic transitions from valence band to conduction band.

Fig. (5C) shows two peaks: the first, at 345 nm, represents the bandgap transitions of ZnO, and the second, at 529 nm, represents the Au NPs peak, which is slightly red shifted compared to the Au NPs alone, ,an additional absorption peak appears at ~262 nm, which can be attributed to interband electronic transitions. The presence of this peak suggests modifications in the electronic structure of ZnO due to the interaction with Au NPs.

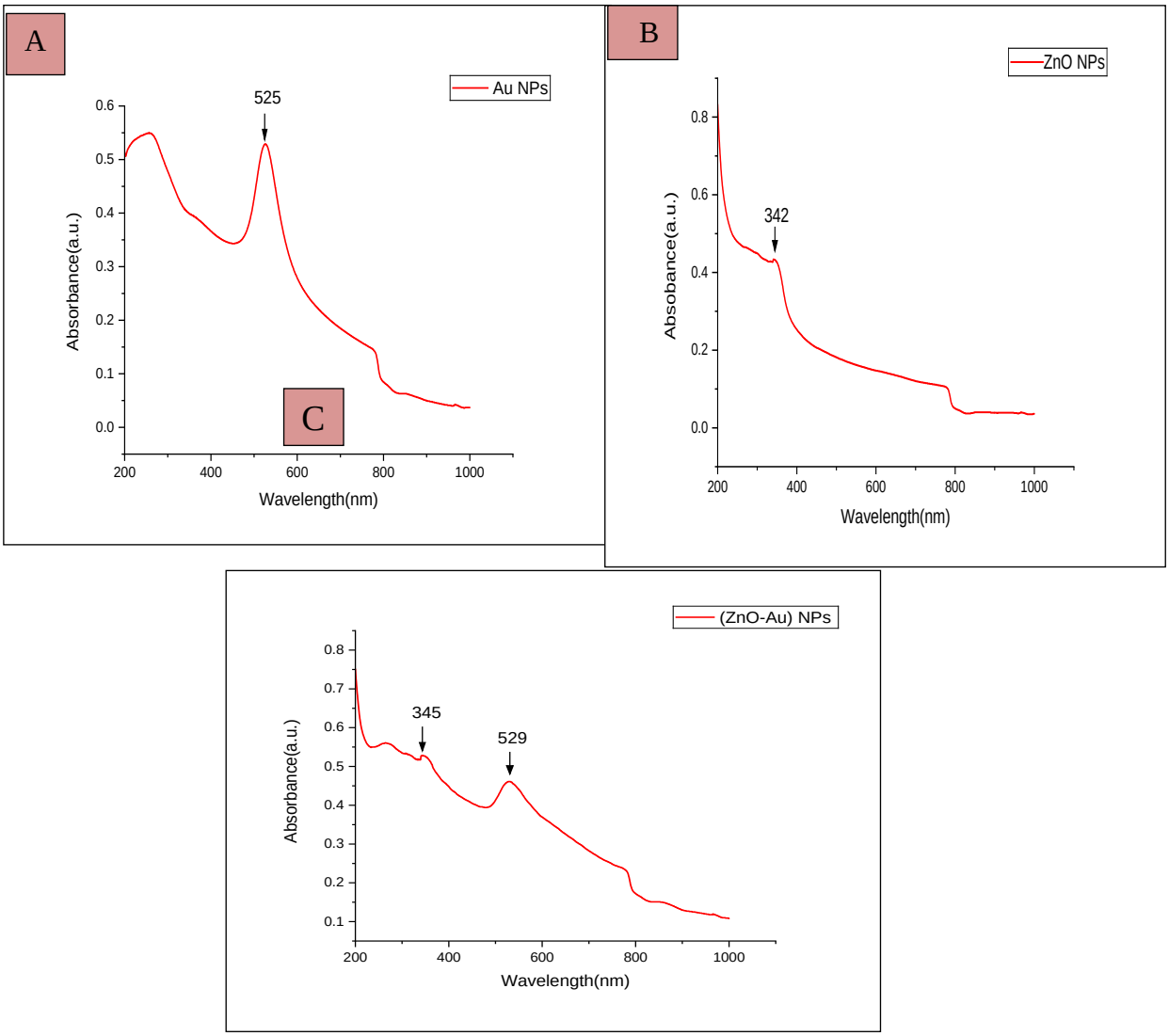

Fig. 5. UV-Visible absorption spectra of Au NPs, ZnO NPs, ZnO-Au nanocomposites.

Fig. (6A) shows that the peak at 3275 cm^{-1} indicates to the O–H stretching vibrations of hydroxyl [OH] groups associated .The band at 1637cm^{-1} indicates C=O vibrations or vibrations of bound water (H–O–H bending), while the band at 2163 cm^{-1} indicates vibrations of C≡C bonds or C≡N bonds . **Fig (6B)** shows that the peak at 3269 cm^{-1} refers O-H stretching vibrations. The band at 1636 cm^{-1} indicates O-H bonding in water molecules adsorbed on the ZnO surface.The band at 2135 cm^{-1} indicates the presence of C≡C (alkynes) or C≡N (nitriles) triple bonds.

Fig (6C) shows that the peak at 3269 cm^{-1} refers O-H stretching vibrations, while the band at 2169 cm^{-1} indicates the presence of C≡C triple bonds (alkynes) or C≡N (nitriles).The peak at 1637 cm^{-1} attributed to O-H-O bond

bending vibrations in absorbed water, or C=O bond vibrations in some organic compounds.

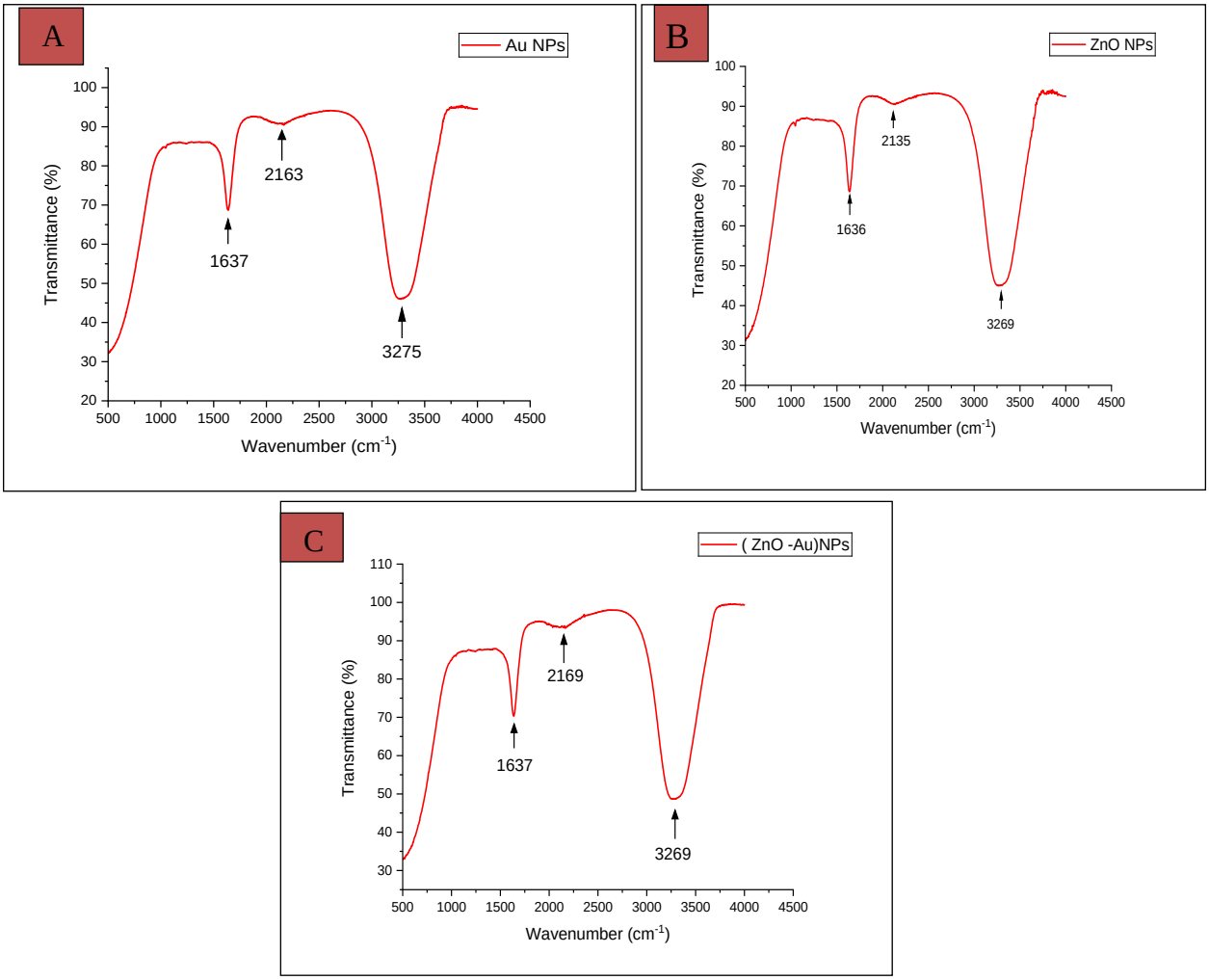

Fig. 6. FTIR spectrum of Au NPs ، ZnO NPs , ZnO-Au nanocomposites.

Fig. (7A) shows the surface morphology of the Au NPs with magnifications 20.00 KX and 50.00 KX and a scale bar of 200 nm. The results indicate that the nanoparticles have an irregular distribution but are clustered in a nearly spherical manner, with pores (voids) between the clusters. The particle size distribution ranges from 18.89 nm to 43.47 nm, indicating a good nanoscale size distribution.

Fig. (7B) shows the surface morphology of the ZnO nanoparticles with 50.00 KX magnifications and a scale bar of 200 nm. The results show that ZnO NPs are an irregular, spherical shape, with obvious agglomeration with particle size distribution ranging from (18.63-46.68) nm.

Fig. (7C) shows the particles typically appear dense, irregularly spherical aggregates, clearly clustered, suggesting aggregated clusters. These agglomerates could result from intense van der Waals forces between the nanoparticles. The particle size distribution ranges from 18.11 nm to 41.4 nm, indicating nanoscale particles.

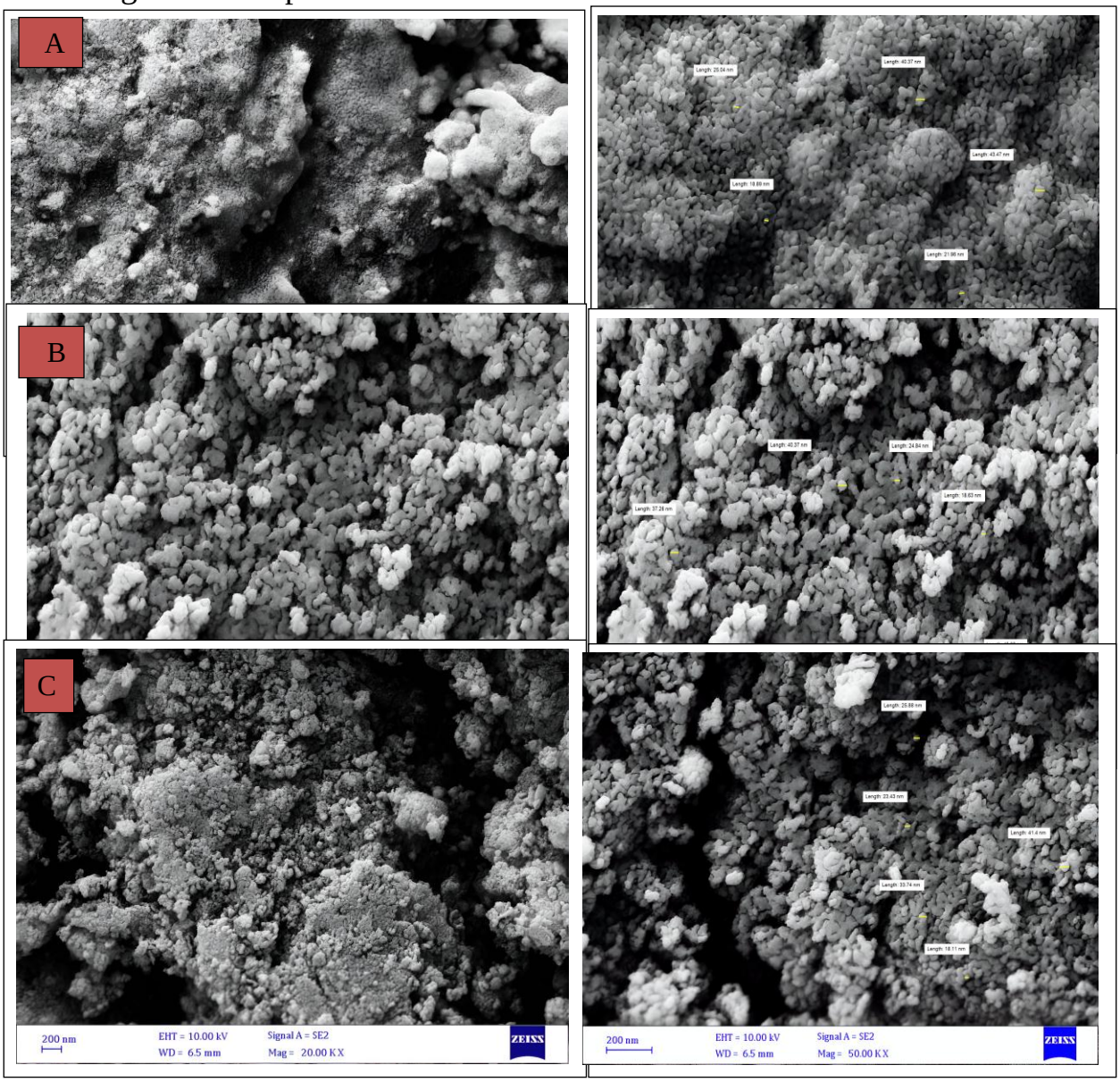

Fig. (8A) shows Au NPs with 100.000 KX magnifications and scale image of 30 nm the Au NPs. The transmission electron microscope image showed that most of the Au NPs had a spherical or sub-spherical shape with observable clumps or aggregates.

Fig. (8B) shows TEM images of ZnO NPs at 45,460× magnification with an 80 nm scale bar. The ZnO nanoparticles appear as darker gray features,

which is attributed to the medium atomic density of Zn relative to Au; consequently, ZnO absorbs and scatters electrons less effectively than heavier Au particles.

Fig. (8C) shows ZnO-Au nanocomposites with 100.000 KX magnifications and scale image of 30 nm, the Dark, spherical particles can be observed distributed over a more transparent, heterogeneous background. The Au particles appear larger and more clearly due to their high density and relatively small number, with some agglomeration , while the ZnO particles appear as a more opaque background and are smaller in size.

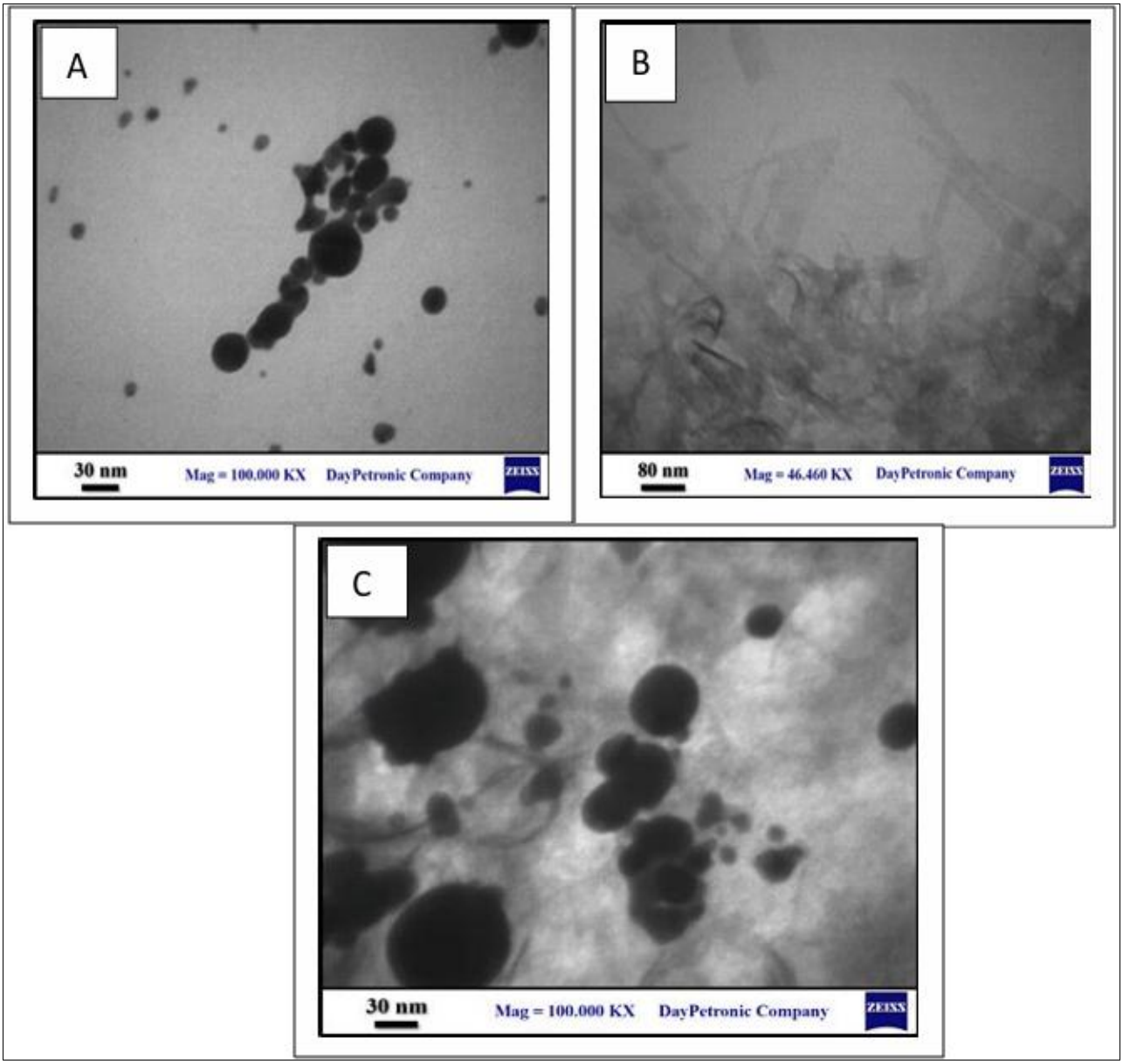

Fig. 8. TEM image of Au NPs ،ZnO NPs, ZnO-Au nanocomposites) .

The open-aperture Z-scan measurements of ZnO-Au nanocomposites were employed to determine the nonlinear absorption coefficient (β), while the closed-aperture configuration was used to extract the nonlinear refractive index (n_2). The corresponding results are summarized in Table 1.

Fig. (9A) a rather weak nonlinear response was noted in the Z-scan curve of Au NPs . This is because Au, being a metallic nanoparticle, shows surface plasmon resonance (SPR) enhancement of light-matter interaction. Nevertheless, nonlinear refraction is not as strong because of the absence of a bandgap as in semiconductors.

Fig. (9B) ZnO nanoparticles evidence a greater nonlinear effect on the Z-scan curve than they contrast at the valley and peak, owing to their property of being wide bandgap semiconductors, which would make their electronic transitions, occur at high intensity light source irradiation. ZnO nanostructures further induce quantum-confinement, which boost the phenomena of nonlinear optically.

Fig.(9C) among the three samples, the ZnO-Au nanocomposites exhibited the highest nonlinear response, likely due to the synergistic interaction between the Au and ZnO components. The surface plasmon resonance (SPR) effect of Au aids in light absorption, while ZnO facilitates charge transfer and electronic transitions, significantly improving the nonlinear optical properties.

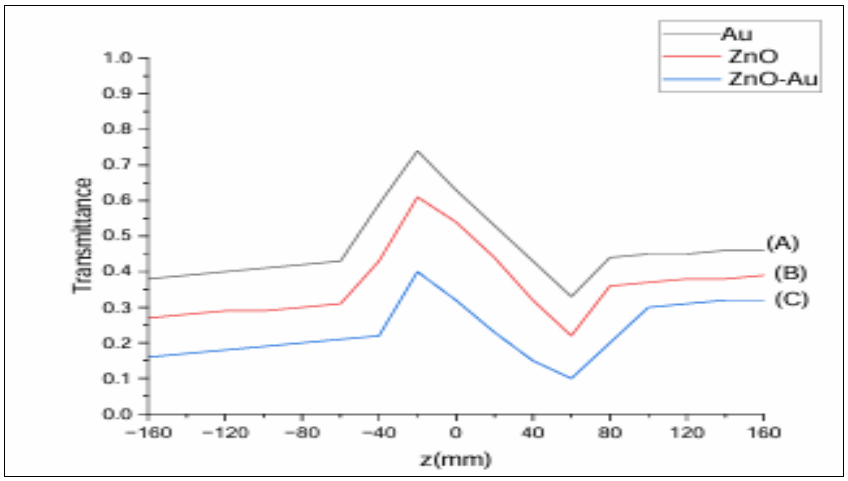

Fig.9. Z-scan of closed aperture of Au NPs, ZnO NPs ،ZnO-Au nanocomposites.

The nonlinear refractive index can be determined from the equation below(Jassim, et al, 2024):

$$n_2 = \Delta\Phi_o / I_o L_{eff}\, k \quad (cm^2/W) \qquad (2)$$

where k: the angular wavenumber equal to ($2\pi / \lambda$), λ is the beam wavelength, $\Delta\Phi_o$ is the nonlinear phase shift, this is calculated by the equation below(Abbas, 2016):

$$\Phi_o = \Delta T_{P-V}/0.406\,(1-S)^{0.25} \quad (3)$$

where L_{eff}: is the effective length of the sample, which can be calculated from the following equation:

$$L_{eff} = (1 - e^{-\alpha_\circ L})/\alpha_0 \ \text{(cm)} \quad (4)$$

where α_0: linear absorption coefficient, L: length of sample, I_o: is the laser beam intensity at focus, given by:

$$I_o = 2P_{peak}/\pi\omega_0 \quad (5)$$

where ω_0 : Radius of beam at focal point, P_{peak}: Laser beam power (W), which can be calculated from the equation below:

$$P_{peak} = E/\Delta t \quad (6)$$

The nonlinear absorption coefficient (β) can be found using the open-aperture Z-scan method from **Eq (7)** (Jassim,et al , 2024).

$$T(z) = \sum_{m=1}^{\infty} \left(\frac{\left(\frac{\beta I\, Leff}{1+\left(\frac{Z}{Z0}\right)^2} \right)^m}{(m+1)^3/2} \right) \quad (7)$$

where Zo: is length of diffraction, m: number integer, Z : position of sample's with minimal transmittance, T(z): minimal transmittance.

Fig. 10. shows Z-scan - open aperture of (Au NPs ،ZnO NPs ،ZnO-Au NCs). All samples exhibited saturated absorption behavior, which is understood from the high transmittance at the focal position (z = 0).This means that the available absorption levels will be filled as the laser intensity at the focal point increases, and thus the absorption decreases.

Fig. (10A) the Au sample showed the lowest peak transmittance value, which suggests a rather weak nonlinear response. This can be explained since Au has plasmonic properties but does not provide sufficient absorption levels on its own at this intensity. In contrast to Au and ZnO,

Fig. (10B) exhibited improved performance, and its semiconducting behavior and wide band gap seem to encourage saturated absorption likely due to the presence of internal energy levels or impurities. The ZnO-Au nanocomposites sample

Fig. (10C) showed the greatest transmittance at the focal point, implying that it had the greatest saturated absorption among the samples. This enhancement was attributed to the hybridization of surface plasmon properties due to the

presence of Au with ZnO structural and electronic properties, thus promoting the electron transfer and light interaction with the system that in turn enhanced the nonlinear effect.

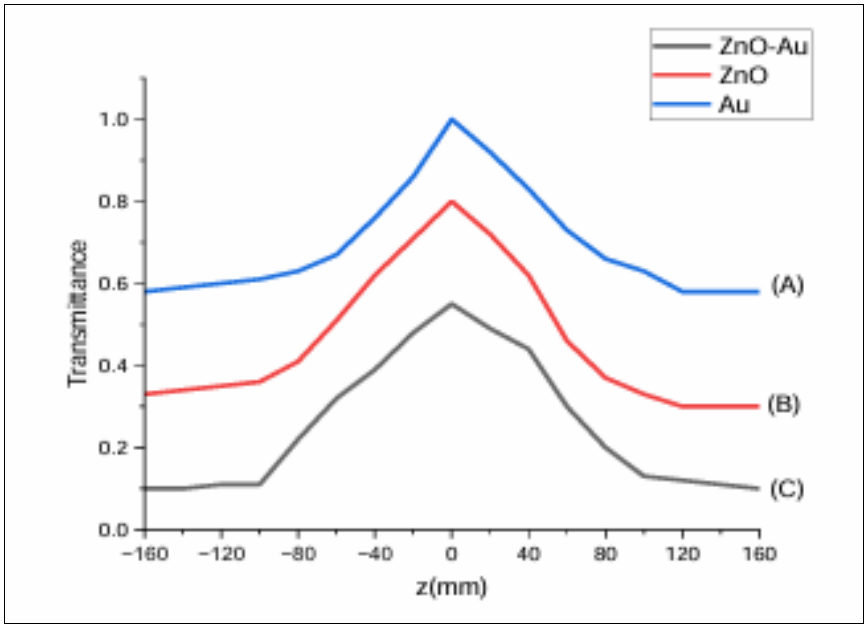

Fig. 10. open aperture Z-scan curves of Au NPs, ZnO NPs, and ZnO-Au NCs.

Table 3. Nonlinear absorption coefficients of nanoparticles using open aperture Z-scan.

Samples	Particle Size (nm)	Tmax	Tmin	ΔTpv	n_2 cm²/GW
Au	30.727	0.74	0.33	0.41	55200
ZnO	27.289	0.61	0.22	0.39	37000
ZnO-Au	27.289	0.4	0.1	0.3	32700

In this study, we employed pulsed laser ablation in liquid (PLAL) to synthesize gold (Au) and zinc oxide (ZnO) nanoparticles and their nanocomposites, focusing on their nonlinear optical properties. Our findings show that the ZnO-Au nanocomposites exhibit enhanced nonlinear optical responses compared to individual ZnO and Au nanoparticles. The nonlinear refractive index (n_2) of ZnO-Au composites was measured at 3.27×10^4 cm²/GW, while the value for ZnO NPs was 3.7×10^4 cm²/GW, and for Au NPs it was 5.52×10^4 cm²/GW. These results suggest that the incorporation of Au into ZnO nanoparticles significantly influences their nonlinear behavior.

Findings of the present research are consistent with the other literature studies, which examined the nonlinear optical characteristics of metal-semiconductor nanocomposites. As an example, Ganeev (2019) reported a substantial improvement of the nonlinear refractive index of ZnO-Au composites over that of pure ZnO, which agrees with our observation. Surface plasmon resonance (SPR) of Au in the composites of ZnO-Au enables a high level of light absorption and the overall enhancement of nonlinear optical properties. On the same note, Walden et al. (2016) established that when the Au nanoparticles are conjugated to ZnO, the nonlinear absorption increases, and this leads to our conclusion that the synergistic effect of Au and ZnO should increase the nonlinear responses. Nevertheless, our work differs slightly in the nonlinear absorption coefficient (β) as our ZnO-Au nanocomposites experienced a lower 0.0650 cm/GW than the values were reported in the work of Walden et al. (2020), who reported higher nonlinear absorption in ZnO-Au hybrids. This variation may be due to the variation in the mode of synthesis or the content of the materials employed in the corresponding studies.

The Z-scan technique that we used is in line with the methods that other authors use to measure nonlinear optical properties (Jassim, 2024). In our study, the Z-scan curves of the Au NPs revealed weak nonlinear response which can be compared with the results of Udayabhaskar et al. (2015) where the authors have observed that the nonlinear refraction due to Au nanoparticles did not play a significant role despite the observation of SPR effects in the same. This may be because Au lacks a bandgap and consequently its nonlinear action is restrictive to that of ZnO. Furthermore, the open-aperture Z-scan measurements of ZnO-Au nanocomposites also demonstrated a high level of saturation absorption, which is also supported by Chen and Hong (2022), who emphasize on the superior absorption

capacity of semiconductor-metal composite. Improved absorption in our ZnO-Au system could be explained by the presence of the two influences of the SPR of Au and the semiconducting nature of ZnO that allow efficient transfer of charges and enhances the absorption cross-section.

In terms of structural properties, XRD and EDX analyses confirmed the successful formation of crystalline ZnO and Au nanoparticles, as well as their nanocomposites. The diffraction peaks observed in our study for ZnO and Au corresponded to standard values, aligning with the findings of Multian et al. (2017), who also reported similar crystallographic peaks for ZnO nanoparticles. The observed particle sizes (30.72 nm for Au NPs, 27.29 nm for ZnO NPs, and 27.29 nm for ZnO-Au NCs) are consistent with the findings of Yao et al. (2021), who reported similar sizes for ZnO-Au nanocomposites synthesized via PLAL. This consistency in particle size and morphology supports the reliability of our synthesis method and confirms the formation of nanoscale materials with high surface-to-volume ratios, which are crucial for their nonlinear optical performance.

The environmental remediation potential of ZnO-Au nanocomposites is another aspect that was explored in our study. Previous studies, such as those by Gündoğdu et al. (2021), have highlighted the photocatalytic applications of ZnO nanomaterials, where their ability to degrade organic pollutants under UV light is enhanced when coupled with noble metals like gold. Our findings suggest that the synergistic effect of ZnO and Au in nanocomposites could indeed offer promising solutions for environmental applications, specifically in the field of water purification and pollutant degradation.

4. Conclusion

Pulsed laser ablation in liquid (PLAL) was used in this study as a surfactant-free method of producing gold nanoparticles (Au NPs), zinc oxide nanoparticles (ZnO NPs), and ZnO -Au nanocomposites (NCs). X-Ray (XRD), transmission electron (TEM), fission energy spectroscopy (FESEM), and energy dispersive X-ray spectroscopy (EDX) structural studies proved the effective development of crystalline and nanoscale materials of different morphology and high purity. The Z-scan technique was used to conduct a systematic study of the nonlinear optical (NLO) properties. ZnO NPs exhibited a nonlinear refractive index (n_2) of 3.7 × 10^4 cm²/GW and a nonlinear absorption coefficient (β) of 0.0823 cm/GW, whereas ZnO–Au NCs showed n_2 = 3.27 × 10^4 cm²/GW and β = 0.0650 cm/GW. These differences show that addition of Au does not affect the robustness of nonlinear responses because of the synergistic interaction between the surface plasmon resonance (SPR) of Au and the semiconducting character of ZnO. In

general, the results suggest ZnO–Au nanocomposites as potential optical limiting and nonlinear photonic devices, and photocatalyst. Also, in this work, the effectiveness of PLAL as a clean, versatile, and reliable process of manufacturing multifunctional nanostructures towards the use in advanced technological applications is confirmed.

References

Abbas, L.A. (2016), "Linear and Nonlinear optical properties of Ag/PMMA nanocomposite films prepared by aerosol assisted Dielectric Barrier Discharge plasma jet polymerization", Technology.

Abdulrahman, H.Z., Ataol, Ç.Y. and Jassim, N.M. (2022), "Plasmonic enhancement in molecular fluorescence of natural curcumin dye with silver nanoparticles synthesis & biological application", Journal of Pharmaceutical Negative Results, Vol. 13 No. 3, pp. 592–603. doi:10.47750/pnr.2022.13.03.088.

Ali, A., Chiang, Y.W. and Santos, R.M. (2022), "X-Ray Diffraction Techniques for Mineral Characterization: A Review for Engineers of the Fundamentals, Applications, and Research Directions", Minerals, Vol. 12 No. 2. doi:10.3390/min12020205.

Chen, L. and Hong, M. (2022), "Functional nonlinear optical nanoparticles synthesized by laser ablation", Opto-Electronic Science, Vol. 1 No. 5, pp. 1–25. doi:10.29026/oes.2022.210007.

Ganeev, R.A. (2019), "Characterization of the Optical Nonlinearities of Silver and Gold Nanoparticles", Optics and Spectroscopy, Vol. 127 No. 3, pp. 487–507. doi:10.1134/S0030400X19090108.

Gündoğdu, Y., Gezgġn, S.Y. and Kiliç, H. (2021), "Effect of Laser Ablation Parameters on Nonlinear Optical Properties of ZnO/Au Nanoparticles", Proceedings of the International Conference on Applied Physics and Mathematics, pp. 8–12. doi:10.17758/eirai10.f1021112.

Jassim, N.M. (2024), "Synthesis and nonlinear optical responses of Ag: ZnO core–shell nanoparticles induced by Z-scan technique", Journal of Optics [Preprint]. doi:10.1007/s12596-024-02432-6.

Jassim, N.M., Ibrahim, N.I. and Khalaf, N.Z. (2024), "Z-scan Study of the Non-linear Optical Properties of Silver/Curcumin Dye Nanocomposites Prepared Via Nanosecond Pulsed Laser Ablation", Revue des Composites et des Materiaux Avances, Vol. 34 No. 4, pp. 533–540. doi:10.18280/rcma.340415.

Mostafa, A.M. (2021), "Preparation and study of nonlinear response of embedding ZnO nanoparticles in PVA thin film by pulsed laser ablation", Journal of Molecular Structure, Vol. 1223, p. 129007. doi:10.1016/j.molstruc.2020.129007.
Multian, V.V. et al. (2017), "Synthesis, Characterization, Luminescent and Nonlinear Optical Responses of Nanosized ZnO", Nanoscale Research Letters, Vol. 12 No. 1. doi:10.1186/s11671-017-1934-y.
Udayabhaskar, R., Divya, T., Ramakrishna, G. and Venugopal Rao, S. (2015), "Nonlinear optical properties of Au–ZnO nanocomposites studied by Z-scan technique", Applied Physics A, Vol. 119 No. 2, pp. 689–696. doi:10.1007/s00339-015-9021-3.
Walden, S.L., Winfield, R.J., McCabe, E.M. and Kelly, J.M. (2016), "Nonlinear absorption of ZnO, ZnO–Au hybrids, and mixed colloids for optical limiting applications", Journal of Nanophotonics, Vol. 10 No. 1, p. 016006. doi:10.1117/1.JNP.10.016006.
Walden, S.L., Winfield, R.J., McCabe, E.M. and Kelly, J.M. (2020), "Nonlinear refractive index of ZnO enhanced by gold nanoparticle coupling", Optical Materials, Vol. 108, p. 110407. doi:10.1016/j.optmat.2020.110407.
Yao, C. et al. (2021), "ZnO:Au nanocomposites with high photocatalytic activity prepared by liquid-phase pulsed laser ablation", Optics and Laser Technology, Vol. 133, p. 106533. doi:10.1016/j.optlastec.2020.106533.
Yogesh, G.K. et al. (2021), "Progress in pulsed laser ablation in liquid (PLAL) technique for the synthesis of carbon nanomaterials: a review", Applied Physics A: Materials Science and Processing. doi:10.1007/s00339-021-04951-6.
Zhang, J. et al. (2017), "Colloidal Metal Nanoparticles Prepared by Laser Ablation and their Applications", ChemPhysChem, Vol. 18 No. 9, pp. 986–1006. doi:10.1002/cphc.201601220.

مجلة كلية التربية الاساسية
كلية التربية الاساسية – الجامعة المستنصرية
Journal of the College of Basic Education Vol.31 (NO. 134) 2025, pp. 48-68

تحضير وخصائص بصرية غير خطية لجسيمات نانوية من الذهب وأوكسيد الزنك ومركباتهما النانوية

نادية محمد جاسم[1]
كلية العلوم، جامعة ديالى، ديالى 4200، العراق.
07712035032
nadiajassim@uodiyala.edu.iq

حنان خالد عوده[2]
كلية العلوم، جامعة ديالى، ديالى 4200، العراق.
07744200031
sciphyms232408@uodiyala.edu.iq

المستخلص

تستعرض هذه الدراسة تحضير الخصائص البصرية غير الخطية لجسيمات نانوية من الذهب (Au) وأوكسيد الزنك (ZnO) ومركباتها النانوية (ZnO-Au NCs)، التي تم تحضيرها باستخدام تقنية الاستئصال بالليزر النبضي في السائل (PLAL). يُعتبر ZnO شبه موصل واسع الفجوة مع طاقة ارتباط إكسيتون عالية (60 ميلي إلكترون فولت)، مما يجعله اقتصاديًا وصديقًا للبيئة وغير سام، وبالتالي مناسبًا للتطبيقات البصرية والإلكترونية. تم إجراء تحليلات للجسيمات النانوية المحضرة باستخدام تقنيات تحليل الأشعة السينية (XRD)، والتحليل الطيفي بالأشعة السينية المشتتة للطاقة (EDX)، والأشعة فوق البنفسجية-المرئية (UV-Vis)، والتحليل الطيفي للأشعة تحت الحمراء باستخدام تحويل فورييه (FTIR)، والمجهر الإلكتروني الماسح (FESEM)، والمجهر الإلكتروني الناقل (TEM). تشير النتائج إلى أن مركبات ZnO-Au النانوية تتمتع بخصائص بصرية غير خطية أفضل من جسيمات Au وZnO الأصلية. تم تحديد معامل الانكسار غير الخطي (n_2) لمركبات ZnO-Au النانوية ليكون 3.27×10^4 سم²/واط، وهو أعلى بكثير من تلك الخاصة بـ ZnO النقي (3.7×10^4 سم²/واط). تم استخدام تقنية Z-scan للحصول على المعاملات البصرية غير الخطية، حيث تبين أن إضافة Au إلى ZnO تزيد من امتصاص الضوء بفضل تأثير الرنين البلازمي السطحي (SPR). تُظهر هذه الدراسة الإمكانات الكبيرة لمركبات ZnO-Au النانوية في تصميم الأجهزة الفوتونية غير الخطية المتقدمة ومعالجة التلوث البيئي، مما يجعلها طريقة نظيفة وفعالة لتحضير المواد النانوية الوظيفية.